Dispersion in acoustic waveguides—A teaching laboratory experiment

K. Meykens[a)]
Limburgs Universitair Centrum, Universitaire Campus, B-3590 Diepenbeek, Belgium
and Limburgs Universitair Centrum, Institute for Materials Research, Materials Physics Division, Universitaire Campus, Wetenschapspark 1, B-3590 Diepenbeek, Belgium

B. Van Rompaey and H. Janssen
Limburgs Universitair Centrum, Universitaire Campus, B-3590 Diepenbeek, Belgium

(Received 5 January 1998; accepted 18 September 1998)

A laboratory experiment for undergraduate students in mathematics and physics is introduced. The experiment concentrates on dispersion in acoustic waveguides. The dispersion relation is measured for different propagation modes and its effect on the transmission of signals is examined, looking at it from several points of view, with the main focus on Fourier aspects. The distortion caused by single mode dispersion is explained in terms of the convolution relation between the input signals and the impulse response of the waveguides. © *1999 American Association of Physics Teachers.*

I. THEORY

When a harmonic acoustic pressure wave, with amplitude p_0 and wave vector $\mathbf{k}$, propagates through a rectangular waveguide, as shown in Fig. 1, the wave can be written as[1]

$$p(x,y,z,t)=p_0\cos(k_y y)\cos(k_z z)\cos(\omega t-k_x x+\phi), \tag{1}$$

where ϕ is the phase constant of the harmonic pressure oscillation at $x=0$.

Although the wave vector $\mathbf{k}$ in Fig. 1 does not point in the x direction, the wave represented by Eq. (1), in fact, travels in the x direction. In the transverse directions, the walls of the waveguide form a resonator cavity, and this turns the transverse wave components into standing waves, as expressed by the amplitude, $p_0\cos(k_y y)\cos(k_z z)$, in wave expression (1). The resonant conditions restrict the wave numbers k_y and k_z to the discrete values

$$k_y=m\,\frac{\pi}{D}\quad\text{and}\quad k_z=n\,\frac{\pi}{W}\quad(m,n\in\mathbb{N}), \tag{2}$$

where D is the height and W the width of the waveguide.

For a given combination m,n in the above expressions for k_y and k_z, the wave is said to propagate in the mode (m,n). A wave may propagate in different modes at the same time.

The instantaneous phase of the wave is $\omega t-k_x x+\phi$. To keep this phase constant, one must travel at velocity ω/k_x. This velocity is known as the *phase velocity* v_p

$$v_p=\omega/k_x. \tag{3}$$

The wave numbers k_x, k_y, and k_z must satisfy the mutually orthogonality equation

$$k_x^2+k_y^2+k_z^2=k^2. \tag{4}$$

Solving the above equation for k_x, and replacing k by its value ω/v, with v the speed of sound in free space, we obtain

$$k_x=[(\omega/v)^2-(m\pi/D)^2-(n\pi/W)^2]^{1/2}, \tag{5}$$

where the expressions (2) have been inserted for k_y and k_z. From this equation can be seen that, unless $m=n=0$, the phase velocity (3) is nonlinearly frequency dependent. This means that only the (0,0) mode is nondispersive, while all the other modes show nonlinear dispersion.

The complex amplitude of the wave is

$$p(x,y,z)=p_0\cos(k_y y)\cos(k_z z)\exp[i(-k_x x+\phi)]. \tag{6}$$

From this complex amplitude can be seen that the wave number k_x must be real valued, as otherwise the wave decays exponentially with x. From Eq. (5) it then follows that the wave can only propagate in a particular mode (m,n) if its frequency exceeds a cutoff value, $\omega_{m,n}$, given by

$$\omega_{m,n}=\pi v\left[\left(\frac{m}{D}\right)^2+\left(\frac{n}{W}\right)^2\right]^{1/2}. \tag{7}$$

The main emphasis of the experiment described below lies on the investigation of the dispersion and its effect on the transmission of signals through the waveguide. In order to examine the effect of dispersion, we consider an arbitrary input signal $f_{\text{in}}(t)$. Its Fourier transform is given by

$$F_{\text{in}}(\omega)=\int_{-\infty}^{\infty}f_{\text{in}}(t)\exp(-i\omega t)\,dt. \tag{8}$$

Now, $F_{\text{in}}(\omega)\in\mathbb{C}$, so it can be written as

$$F_{\text{in}}(\omega)=|F_{\text{in}}(\omega)|\exp[i\phi_{\text{in}}(\omega)], \tag{9}$$

where $\phi_{\text{in}}(\omega)$ is the phase constant of the harmonic components which make up the input signal. The harmonic components can alternatively be written in the form of the complex amplitude (6). The phase constant $\phi_{\text{in}}(\omega)$ then corresponds to $-k_x x+\phi$, evaluated at the entrance position $x=x_{\text{in}}$ of the waveguide. In what follows, the entrance position will be taken as $x_{\text{in}}=0$.

If absorption can be neglected, the amplitude spectrum $|F_{\text{in}}(\omega)|$ remains unchanged with propagation. The phase factor in expression (9), however, is not conserved but changes with x according to $\exp[i(-k_x(\omega)x+\phi_{\text{in}}(\omega))]$. The Fourier transform of the output signal, measured at any position x down the waveguide, is thus given by

$$F_{\text{out}}(\omega,x)=F_{\text{in}}(\omega)\exp[-ik_x(\omega)x]. \tag{10}$$

In the nondispersive case of mode (0,0), k_x is linearly proportional to ω, according to Eq. (5)

$$k_x=\omega/v. \tag{11}$$

With k_x linearly proportional to ω, the phase shift in Eq. (10) causes a distortion-free translation in the time domain, according to the Fourier transform property[2]

 © 1999 American Association of Physics Teachers

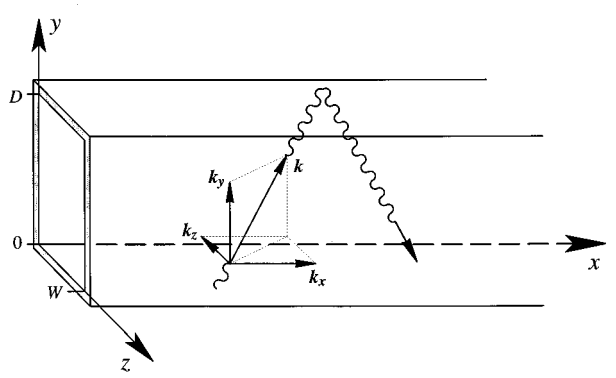

Fig. 1. Three-dimensional waveguide with coordinate system and dimensions.

$$\mathcal{F}[f_{\text{in}}(t-t_0)]=\mathcal{F}[f_{\text{in}}(t)]\exp(-i\omega t_0), \tag{12}$$

where $\mathcal{F}$ stands for Fourier transform and where t_0 corresponds to x/v, according to the combined equations (10) and (11).

In general, the output signal is given by the inverse Fourier transform of formula (10). In the time domain this corresponds to the convolution of the input signal with the inverse transform, $\mathcal{F}^{-1}$, of the phase delay function $\exp(-ik_x(\omega)x)$,

$$f_{\text{out}}(t,x)=f_{\text{in}}(t)\otimes\mathcal{F}^{-1}[\exp(-ik_x(\omega)x)], \tag{13}$$

where $\otimes$ stands for convolution product.

Considering the waveguide to be a linear time-invariant transmission system, the output signal can be written as[3] the convolution product of the input signal with the impulse response of the transmission system

$$f_{\text{out}}(t,x)=f_{\text{in}}(t)\otimes h(t), \tag{14}$$

where $h(t)$ stands for the impulse response. Comparing this transmission relation with Eq. (13), one finds that the impulse response of the waveguide is given by

$$h(t,x)=\mathcal{F}^{-1}[\exp(-ik_x(\omega)x)]. \tag{15}$$

In mode (0,0) the impulse response can easily be calculated and is equal to

$$h(t,x)=\delta(t-x/v). \tag{16}$$

A convolution with a δ-function causes no distortion on $f_{\text{in}}(t)$. It simply shifts the input signal in time, in accordance with the above-mentioned Fourier transform property.

Now, we would like to see what the impulse response (15) looks like in mode (1,0). In this case, the wave number k_x is not linearly proportional to ω, but, according to formula (5),

$$k_x=[(\omega/v)^2-(\pi/D)^2]^{1/2}. \tag{17}$$

Inserting this expression into Eq. (15), an approximate (1,0) impulse response can be calculated. Figure 2 shows a numerically calculated (1,0) impulse response for $x=3$ m and $D=0.142$ m. For comparison, the numerically calculated (0,0) impulse response is also shown.

Where the (0,0) approximation in Fig. 2 approaches a Dirac δ-function fairly well, the (1,0) impulse response looks more like a δ-function from which the low frequencies have escaped into a (reversed) chirplike trailing edge.

We will look more closely into the distorting effect of the (1,0) impulse response presently.

II. EXPERIMENTAL SETUP

The experimental setup, used in the students laboratory, is shown schematically in Fig. 3. The waveguide of the setup is a commercially available, 6 m long aluminum pipe with a rectangular cross section of size $D=0.142$ m and $W=0.05$ m.

The lowest cutoff frequencies corresponding to these cross-sectional dimensions are, in order of increasing frequency [cf. Eq. (7)]: $\omega_{0,0}=0$ rad s^{-1}, $\omega_{1,0}=2\pi\times1200$ rad s^{-1}, $\omega_{2,0}=2\pi\times2400$ rad s^{-1}, $\omega_{0,1}=2\pi\times3400$ rad s^{-1}, $\omega_{3,0}=2\pi\times3600$ rad s^{-1},… . Throughout the experiment the wave frequency will be kept well below the $\omega_{0,1}$ cutoff, thus restricting the allowed propagation modes to $(m,0)$ modes only, with $m=0,1,2$.

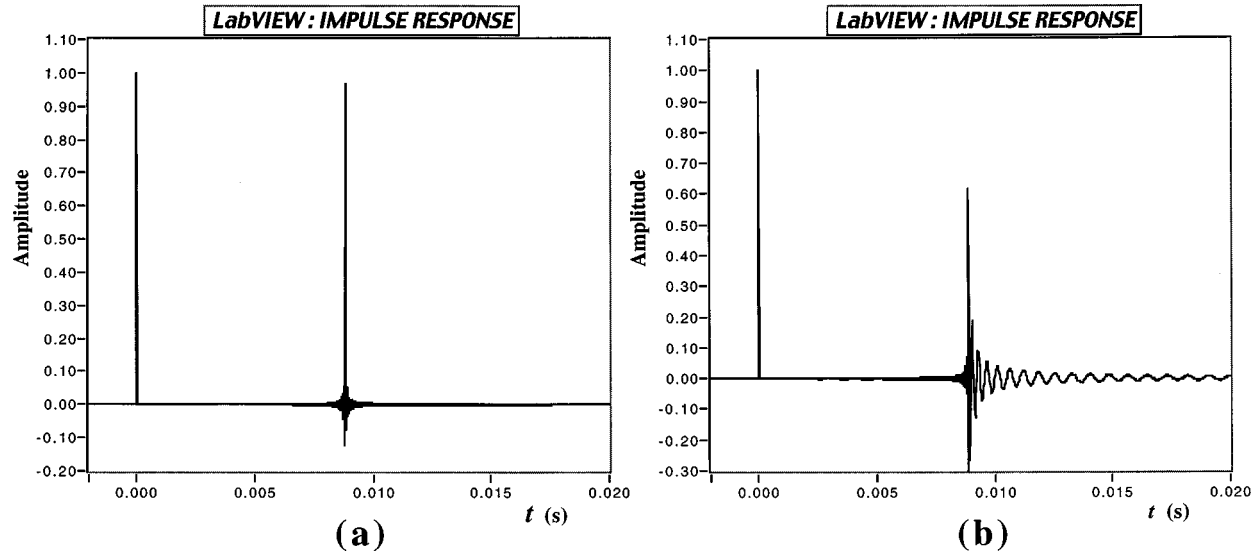

Fig. 2. Unit input impulses ($t=0$) and the numerically calculated impulse responses at $x=3$ m in a rectangular acoustic waveguide with cross-sectional dimensions $D=0.142$ m and $W=0.05$ m (cf. Fig. 1). (a) Propagation mode (0,0). (b) Propagation mode (1,0).

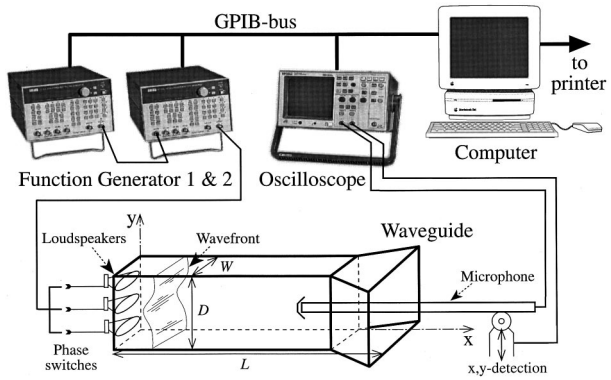

Fig. 3. Experimental setup. An acoustic (2,0) pressure front is represented inside the wave guide.

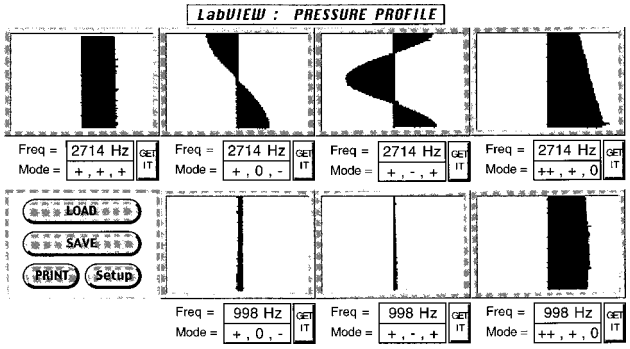

Fig. 4. Acoustic pressure profiles corresponding to the indicated frequencies and settings of the speakers. (The setting $[++,+,0]$ stands for $[2+,+,0]$.) The profiles are measured at $x=3$ m down the laboratory waveguide. The vertical axis on the figures corresponds to the y position across the waveguide. The pressure amplitudes are displayed in horizontal direction, left or right from the middle according to the relative phase of the pressure oscillations.

At the entrance of the waveguide three loudspeakers are mounted side by side along the y axis. They are driven by the same function generator. Its output amplitude can be modulated by means of an external modulation source. For that purpose an auxiliary function generator is provided. Both function generators are programmable (Thurlby, Thandar, TTi TG1304) and can be linked up to a computer. The leads between the main function generator and each of the speakers can be interchanged separately, thereby introducing a phase shift of 180 deg. The notation $+$ or $-$ will be used to indicate the relative phases of the speakers, e.g., the indication $(+,0,-)$ means that the two outer speakers move in phase opposition with each other, while the symbol 0 means that the middle speaker is disconnected. The relative amplitudes of the speakers can also be adjusted. They will be indicated by numbers in front of the phase symbols (the number 1 will be omitted), e.g., $(2+,0,-)$ means the same phase relation as $(+,0,-)$ but with the amplitude of the $+$ speaker twice the amplitude of the $-$ speaker.

The relative phases and amplitudes of the speakers tailor the acoustic wave front along the y axis at the entrance of the waveguide. Different modes $(m,0)$ can thus be generated, as will be examined in the first part of the experiment.

The acoustic pressure field inside the waveguide can be gauged by means of a small microphone. The microphone is mounted on an x,y-translation stage and its position is detected electronically by means of two potentiometers.

The microphone signal is applied to a digital storage oscilloscope (HP 54600) where it can be visualized and preconditioned before being transferred to a computer (Power Macintosh).

The oscilloscope and the function generators are linked up to the computer by means of a General Purpose Interface Bus (GPIB IEEE 488).

A number of LabVIEW™ application programs have been custom developed. They are designed to read the signals from the oscilloscope into the computer and to carry out the analysis of these signals according to the requirements of the experiment.

The reader who wants to know more about these LabVIEW™ applications may contact the authors for full information and free copies of the programs.

III. EXPERIMENTAL RESULTS

A. Propagation modes

In order to investigate the propagation modes generated by different phase and amplitude settings of the speakers, continuous sine waves are applied to the waveguide. For each setting of the speakers, the amplitude pattern of the wave is measured at a distance $x=3$ m down the waveguide. Figure 4 shows some of the patterns recorded by the students.

The amplitude pattern corresponding to a particular setting of the speakers is measured at different wave frequencies, either above and below the different cutoffs. Each setting can thus be checked to determine whether it generates single- or multimodes. From Fig. 4, it can be seen that the settings $(+,+,+)$, $(+,0,-)$, and $(+,-,+)$ generate single modes only. The setting $(2+,+,0)$, however, generates the double mode $(0,0)+(1,0)$, provided the wave frequency is above the $\omega_{1,0}$ cutoff.

It is interesting to note that the $(2+,+,0)$ amplitude pattern does not look like a straightforward superposition of the patterns (0,0) and (1,0), although it was tailored that way by the speakers at the entrance of the waveguide. The initial tailoring, however, is not conserved with propagation, because of the different phase velocities of the modes (0,0) and (1,0). The difference in phase velocity makes the phase relation between the two modes x dependent, and this, in turn, makes the superposition amplitude pattern change with propagation.

B. Dispersion relation $\omega=\omega(k_x)$

The dispersion relation $\omega=\omega(k_x)$ can be obtained from Eq. (5). A graphical presentation of this relation is shown in Fig. 5(a), for the modes $(m,0)$ with $m=0$, 1, 2 respectively.

Figure 6 shows a number of experimentally obtained (ω,k_x)-points. The data points were obtained by moving the microphone, at each of the selected frequencies, inside the waveguide over a distance Δx while watching the phase shift $\Delta\varphi$ of the microphone signal on the oscilloscope screen. Measuring both $\Delta\varphi$ and Δx, k_x could be obtained using the relation $|\Delta\varphi|=k_x|\Delta x|$, according to the phase factor of the complex amplitude in expression (6). In Fig. 5(b), the experimental (ω,k_x)-points are superimposed on the theoretical curves of Fig. 5(a).

C. Signal transmission

In order to investigate the transmission of signals through the waveguide, the continuous sine waves, used up to this

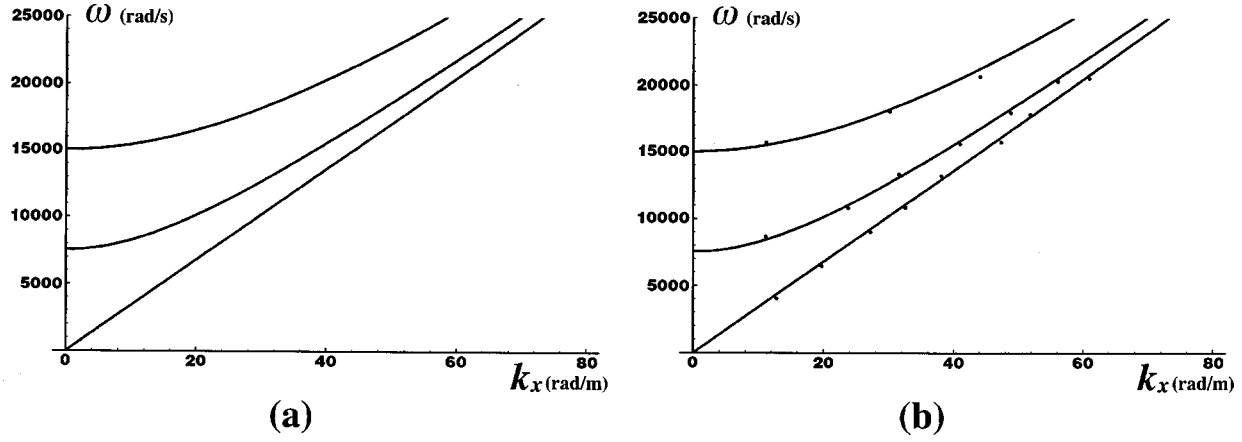

Fig. 5. Dispersion curves for the laboratory acoustic waveguide. (a) Theoretical plots according to Eq. (5). (b) Superposition of the experimental data points of Fig. 6 on the theoretical plots.

point in the experiment, are now amplitude modulated into discrete short wave trains. To start with, 5 ms long 1500 Hz wave trains with a triangular amplitude envelope, as shown in the top trace of Fig. 7, are applied to the waveguide. A triangular, rather than a rectangular amplitude envelope is chosen to assure an envelope maximum which is well defined in time. This makes it easier to follow the propagation of the signals, as will be explained in Sec. III C 2. (The mathematically simpler Gaussian profile could not be obtained from the function generators.)

Later in the experiment the students may change any of the parameters (length, carrier frequency, envelope) of the wave trains to examine the effect on the transmission characteristics.

Figure 7 shows, besides the initial input signal, the corresponding output signals at $x=3m$ in the single modes (0,0) and (1,0) and in the double mode $(0,0)+(1,0)$ respectively. These signals will be discussed in the next sections.

1. Frequency analysis

From Fig. 7, it can be seen that the periodicity within the (1,0) output signal is not constant. The number of periods per time division (5 ms) of the oscilloscope screen decreases from about 8 in the time interval [10.0, 15.0] ms to 7 in the interval [15.0, 20.0] ms and further down to 6.5 in the interval [20.0, 25.0] ms. The corresponding frequencies range from 1600 Hz, through 1400 Hz, down to 1300 Hz, while the carrier frequency was set on 1500 Hz. This spectrum of frequencies manifests the line broadening caused by the amplitude modulation. The fact that these different frequencies are discernible in the (1,0) signal but neither in the input signal nor in the (0,0) output signal has to do with the dispersion in the (1,0) propagation mode, as will be explained in Sec. III C 3.

The line broadening caused by the amplitude modulation of the 1500 Hz sine wave can, however, always be visualized by taking the Fourier transform of the signals. Figure 8 shows the FFT-amplitude spectra of the input signal and of the (1,0) output signal of Fig. 7, respectively. The main difference between these two spectra is the missing left side lobes in the (1,0) spectrum. This is due to the fact that these side lobes lie below the $\omega_{1,0}$ cutoff frequency.

Fourier spectra, such as those in Fig. 8, do not reveal any time localization of the frequencies within a signal. To obtain a joint time-frequency analysis, one can subdivide the signal into pieces of length Δt and then take the Fourier transform of the successive pieces. This method is known as slit Fourier transform (FFT slit) or short-time Fourier transform (STFT).

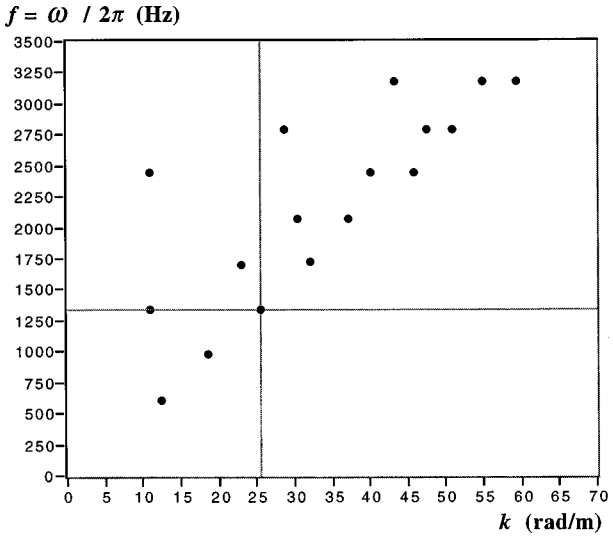

Fig. 6. Experimentally recorded ω, k_x-data points. These data points are to be compared with the theoretical dispersion plots of Fig. 5(a).

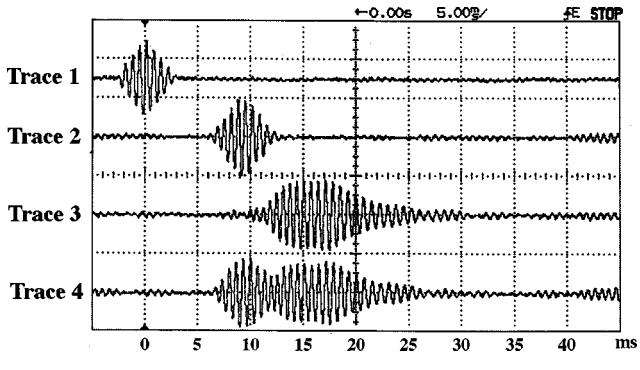

Fig. 7. Input signal (Trace 1) and the corresponding output signals in mode (0,0) (Trace 2), (1,0) (Trace 3), and $(0,0)+(1,0)$ (Trace 4), respectively, measured at $x=3$ m in the laboratory waveguide.

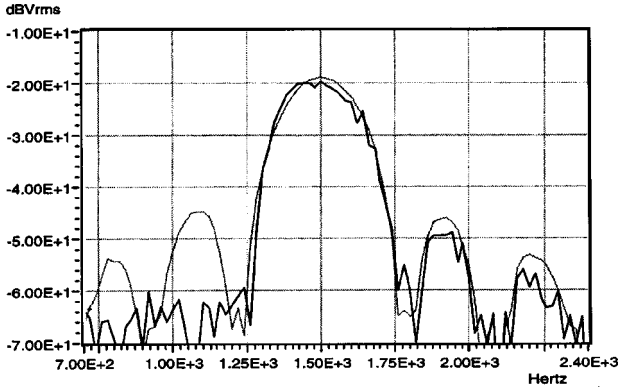

Fig. 8. Fourier amplitude spectra of the input signal (light) and (1,0) output signal (dark) shown in Fig. 7.

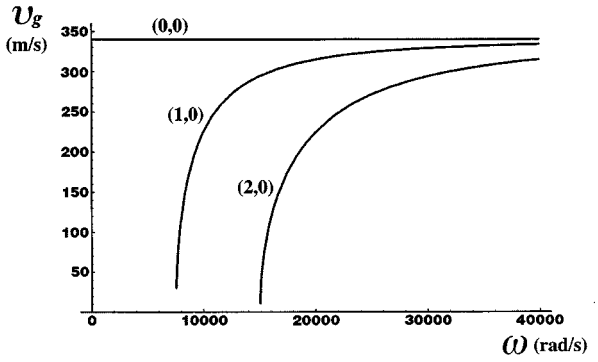

Fig. 10. Group velocity versus frequency for the propagation modes (0,0), (1,0), and (2,0), respectively, in the laboratory waveguide.

The details of STFT fall outside the scope of this laboratory experiment and the students are referred to more advanced courses in signal analysis (e.g., Ref. 4) for further information about joint time-frequency transform methods. However, they should realize that, according to the uncertainty principle $\Delta\nu = 1/\Delta t$, sharpness of the time analysis has to be traded off for sharpness in frequencies, and vice versa.

Figure 9 shows a STFT amplitude spectrum of the (1,0) signal of Fig. 7. It gives a good estimate of the time of arrival, at $x = 3$ m, of the different frequencies which make up the (1,0) signal. From this spectrum, the group velocity can be determined, as will be discussed in the next section.

2. Group velocity

When dispersion occurs, the appearance of a signal may change drastically with propagation. It may then be difficult to define any significant single velocity for this signal. If, however, there is only a small amount of dispersion over the frequency band of interest, the overall shape of the signal may stay recognizable over a long distance. The signal velocity can then be taken as the speed of propagation of the signal envelope maximum. This velocity is called the *group velocity* v_g and can be obtained from the dispersion relation (5) by using the relationship[5]

$$v_g = \frac{d\omega}{dk_x}, \tag{18}$$

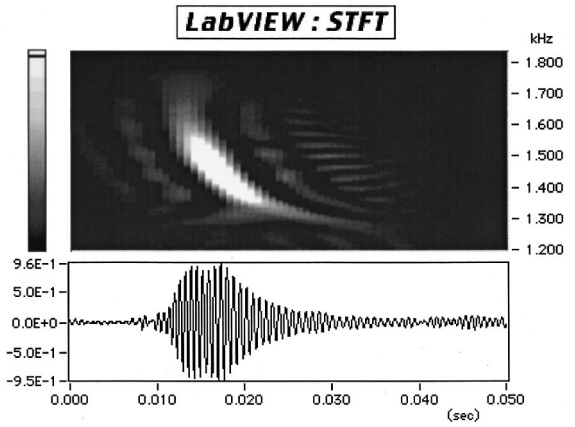

Fig. 9. Joint time-frequency spectrum (STFT) of the (1,0) output signal shown in Fig. 7.

where the derivative must be evaluated at the center frequency of the Fourier spectrum of the signal.

In Refs. 1, 6, and 7, excellent explanations are given of the physical meaning of the group velocity in waveguides. In this paper, however, we do not look into these explanations but restrict ourselves to the frequency dependence of the group velocity as it may be derived from the dispersion relation (5).

Two graphical interpretations of formula (18) are helpful to see how the group velocity changes with frequency. First, the slope of the tangent line on the dispersion curves in Fig. 5(a) is a direct indicator of the frequency dependency of v_g and need no further comment. Second, calculating $d\omega/dk_x$ from the dispersion relation (5) shows that the group velocity can be written as $v_g = v\cos\theta$, with θ the angle the wave vector **k** in Fig. 1 makes to the x axis. Now, for a given mode, the y,z components of the wave vector are fixed. The total length of the wave vector, however, changes with frequency, according to $k = \omega/v$. Thus, in any of the propagation modes but (0,0), the angle θ must change with frequency, from almost 90° near cutoff to 0° in the limit of infinitely high frequencies. The corresponding group velocity changes from almost zero to the speed of sound in free space.

Figure 10 gives a quantitative picture of the group velocity versus frequency for some of the modes in the waveguide used in the students laboratory.

The triangular shape of the input signal in Fig. 7 is sufficiently recognizable in the (1,0) signal to allow the use of formula (18) to determine the propagation velocity of the (1,0) signal. From Fig. 7 can be seen that the time of arrival, at $x = 3$ m, of the (1,0) envelope maximum is approximately 16 ms. The corresponding group velocity is 190 ms^{-1}, where the theoretical group velocity at $\omega = 2\pi \times 1500$ rad s^{-1} is 200 ms^{-1}, according to Fig. 10.

Instead of the single time of arrival of the signal as a whole, as obtained above from the envelope maximum, a more detailed picture of the time of arrival of the signal is given by the joint time-frequency plot of Fig. 9. There, the time of arrival is shown as a function of frequency within the frequency band of the signal.

Estimating the time of arrival at a given frequency from the time that frequency reaches its intensity maximum on the STFT spectogram of Fig. 9, the time of arrival at 1500 Hz can be seen to be about 16 ms. This is in accordance with the time of arrival of the envelope maximum of the (1,0) output signal in Fig. 7. Frequencies near the (1,0) cutoff have a much delayed time of arrival, e.g., 1300 Hz can be seen to be

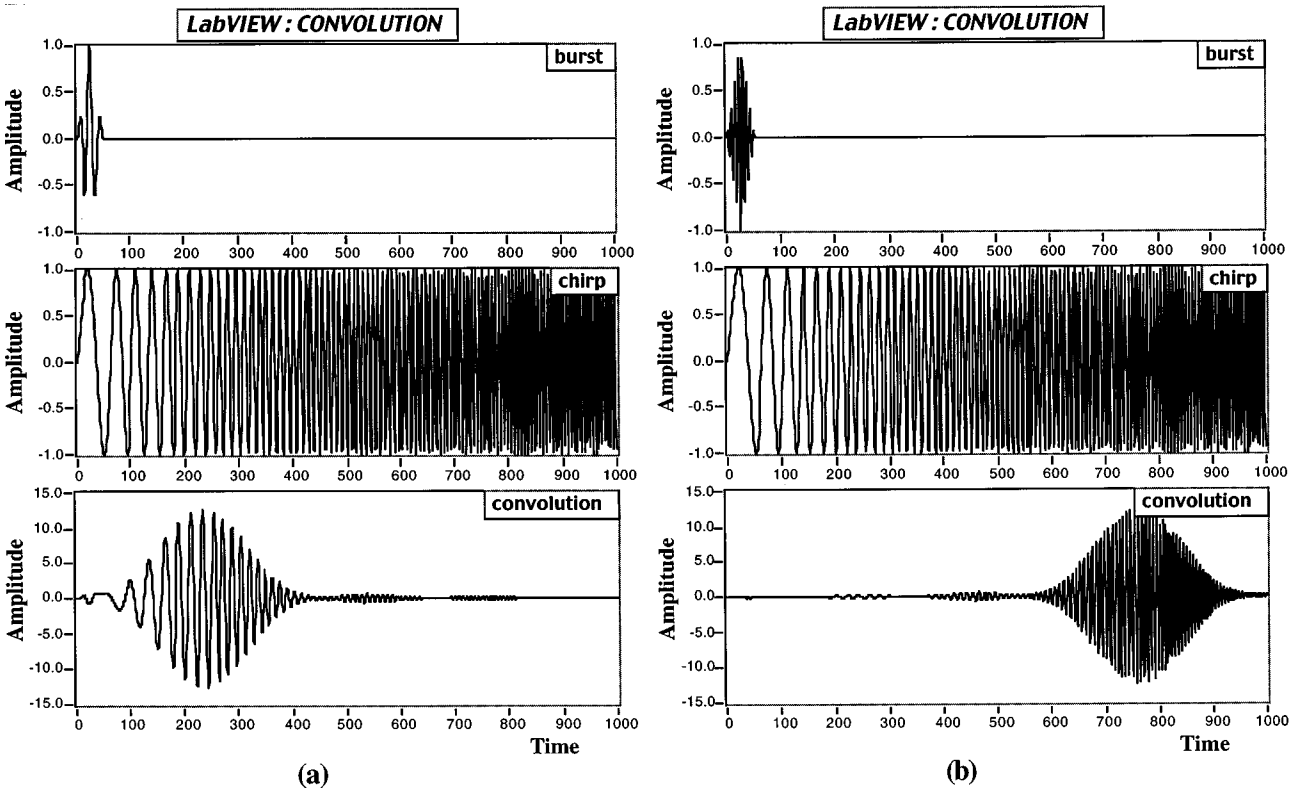

Fig. 11. Convolution of a triangular sine burst with a chirp-function. The convolution shows a maximum at the points in time where the frequencies within the spectrum of the burst coincide with the frequencies of the chirp-function. (a) Sine frequency near the start frequency of the chirp. (b) Sine frequency near the end of the chirp.

localized in time at approximately 27 ms. This latter corresponds to a group velocity $v_g = 110\ \mathrm{ms}^{-1}$, where, according to Fig. 10, the theoretical value at 1300 Hz is 130 ms^{-1}.

3. Distortion

The distortion of the output signals (1,0) and (0,0) $+$(1,0), relative to the input signal in Fig. 7, is caused mainly by dispersion. The (1,0) signal is distorted by single-mode dispersion only, while the (0,0)$+$(1,0) suffers an additional distortion from the intermodal dispersion between the propagation modes (0,0) and (1,0). In this section we will look into the distortion caused by single-mode dispersion only.

As mentioned at the beginning of Sec. III C, the students may change any of the parameters (length, carrier frequency, envelope) of the input signal to examine the effect on the transmission characteristics. Their main findings are (i) the distortion of the (1,0) output signal decreases when the carrier frequency is moved away from the cut-off edge, (ii) the distortion decreases when the input signals are made longer, and (iii) the distortion becomes worse when the input signal envelope is changed from a triangular into a rectangular shape.

It is interesting to explain the distortion and the above-mentioned findings in terms of the convolution relation (14), according to which the output signal is the convolution of the input signal with the impulse response of the waveguide.

The (1,0) impulse response of the waveguide is shown in Fig. 2(b). As mentioned in the context of Fig. 2(b), this impulse response looks like a reversed chirplike function, with the high frequencies compressed into a Dirac δ-like leading edge.

A convolution may be compared[6] to a correlation function and, just as a cross correlation measures the similarity between two functions, so does the convolution (16), as a function of time, show a maximum when the frequencies of the input signal recognize themselves in the response function. This is demonstrated in Fig. 11. The signals in Fig. 11 are computer simulations of triangular wave trains convolved with a chirp function. The triangular wave trains are centered around $t=0$. The convolutions show a maximum when the chirp function reaches the wave train frequencies or, in other words, when the wave train frequencies match the chirp frequency.

The distortion can now be explained by positioning the signal frequencies on the chirplike impulse response in Fig. 2(b). High frequencies of the input signal will find themselves back in the δ-function-like leading edge. So, when only high frequencies are involved in the input signal, the low-frequency tail of the impulse response has little effect. The δ-like leading edge of the impulse response introduces only little distortion. (An exact δ-function introduces no distortion at all.) Lower frequencies, however, tend to move the center of gravity of the convolution towards the low-frequency tail of the response function, thus smearing the output signal in time and giving its envelope maximum an extra delay.

Now, the above-mentioned findings of the students can easily be explained. An increase of the carrier frequency shifts the position of the signal frequencies on the impulse response towards the δ-like leading edge, thus decreasing the overall distortion of the output signal. Shortening the output signals or changing their amplitude envelope from triangular to rectangular both widen the Fourier spectrum of the sig-

nals. Lower frequencies are thus introduced and this, in turn, enhances the distorting effect of the tail of the impulse response.

IV. CONCLUSION

Although the intuitive approach to the Fourier aspects involved in the above-described laboratory experiment is highly appreciated by the students, we are aware that the experiment itself may look a bit artificial, with little practical relevance. As is made clear in, e.g., Refs. 8 and 9, however, the concepts encountered in the above experiment are of actual interest in modern technology.

To enhance the relevance, the extrapolation route to optical fiber telecommunication is pointed out to the students. In particular, the acoustic waveguide may be compared to a step-index fiber. The physics behind a number of problems, such as, e.g., the restriction of the transmission rate due to dispersion in fiber telecommunication, can adequately be understood from the acoustic waveguide.

ACKNOWLEDGMENTS

The authors are most indebted to R. Lempens and D. Przybylski for their invaluable help in designing and developing the LabVIEW™ applications used in the experiment. Most of the computer programming and the computerization of the measuring equipment was done by them. The authors also thank J. Soogen, who constructed the waveguide of the experimental setup. B. Van Rompaey acknowledges financial support from FWO, Flanders (Belgium), as a research assistent.

[a)]Electronic mail: kristien.meykens@luc.ac.be

[1]K. Uno Ingard, *Fundamentals of Waves and Oscillations*, 2nd ed. (Cambridge U.P., Cambridge, England, 1990).
[2]Hwei P. Hsu, *Fourier Analysis*, Simon and Schuster Tech Outlines (Simon and Schuster, New York, 1970).
[3]L. R. Rabiner and B. Gold, *Theory and Application of Digital Signal Processing* (Prentice–Hall, Englewood Cliffs, NJ, 1975).
[4]M. Vetterli and J. Kovačevič, *Wavelets and Subband Coding* (Prentice–Hall, Englewood Cliffs, NJ, 1995).
[5]Stephen G. Lipson, Henry Lipson, and David S. Tannhauser, *Optical Physics*, 3rd ed. (Cambridge U.P., Cambridge, England, 1995).
[6]K. Iizuka, *Engineering Optics*, 2nd ed. (Springer-Verlag, Berlin, 1987).
[7]F. S. Johnson, ''Physical cause of group velocity in normally dispersive, nondissipative media,'' Am. J. Phys. **58**, 1044–1056 (1990).
[8]R. Szipocs and A. Kdrazikis, ''Theory and design of chirped dielectric laser mirrors,'' Appl. Phys. B: Lasers Opt. **65** (2), 115–135 (1997).
[9]A. Macleod, ''Coatings for ultrafast applications,'' Second Workshop of European Vacuum Coaters, Amzio, Ce.Te.V., Carsoli (AQ), Italy (1996).

THE VALUE OF MATHEMATICAL LIFE

I have never done anything 'useful'. No discovery of mine has made, or is likely to make, directly or indirectly, for good or ill, the least difference to the amenity of the world. I have helped to train other mathematicians, but mathematicians of the same kind as myself, and their work has been, so far at any rate as I have helped them to it, as useless as my own. Judged by all practical standards, the value of my mathematical life is nil; and outside mathematics it is trivial anyhow. I have just one chance or escaping a verdict of complete triviality, that I may be judged to have created something worth creating. And that I have created something is undeniable: the question is about its value.

G. H. Hardy, *A Mathematician's Apology* (Cambridge University Press, 1969; reprint of 1940 edition), pp. 150–151.